

Characterization of xanthan solutions for application in EOR

W. M. Kulicke, R. Oertel, M. Otto, W. Kleinitz, W. Littmann

*W. M. Kulicke, R. Oertel, M. Otto
Institut für Technische und Makromolekulare Chemie, Universität Hamburg, Bundesstraße 45, D-2000 Hamburg 13*

*W. Kleinitz, W. Littmann
PREUSSAG Erdöl und Erdgas GmbH, Karl-Wiechert-Allee 4, D-3000 Hannover 61*

Characterization of xanthan solutions for application in EOR

W. M. Kulicke, R. Oertel, M. Otto, W. Kleinitz, W. Littmann

Ultrahochmolekulare Polymere in niedrig konzentrierter Lösung gewinnen in der tertiären Erdölförderung zunehmend an Bedeutung. Während Polyacrylamid-co-acrylate in Lagerstätten mit geringem Salzgehalt Verwendung finden, kann Xanthan auch bei höheren Salzgehalten eingesetzt werden. In dieser Studie wurden die folgenden Eigenschaften des Xanthans detailliert untersucht; intrinsische Viskosität, Molmasse, Fließverhalten, Viskositätsergiebigkeit und der Gehalt an Acetat- und Pyruvatgruppen (NMR und enzymatische Analyse). Die Ergebnisse zeigen, daß sich die verschiedenen Xanthan-Proben in Bezug auf ihre Viskosität und Injizierbarkeit unterscheiden. Dies erklärt die oft voneinander abweichenden publizierten Daten über Xanthan, wie z. B. $[\eta]$ - M -Beziehungen. Es konnte gezeigt werden, daß diese Unterschiede mit den unterschiedlichen Acetat- und Pyruvatgehalten korrespondieren. Dies bedeutet, daß Xanthan als ein kompliziertes Quartär-Polymer betrachtet werden muß. Die Lösungsstruktur (Konformation) muß als aufgeweitetes Knäuel und nicht als starres Stäbchen betrachtet werden.

Ultra-high molecular weight polymers in low concentrated solution have been attracting an increasing degree of significance for use in enhanced oil recovery. Polyacrylamide-co-acrylates are used in reservoirs with a low salt content, whereas xanthan can be employed in reservoirs with a high salt content. In this study the following characteristics of xanthan were investigated in detail; intrinsic viscosity, molecular weight, flow behaviour, viscosity yield, and degree of acetate and pyruvate substitution (NMR and enzymatic analysis). The results show that the various xanthan samples differ from one another with respect to their viscosity and injectability. This therefore explains the often contradictory data on xanthan, such as the $[\eta]$ - M -relationship, which is found in publications. It was possible to show that these differences may well be connected with the varying pyruvate and acetate contents, which mean that xanthan may be regarded as a complicated quaternary polymer. The solution structure (conformation) must be regarded as an extended coil and not as a rigid rod.

1. Introduction

Because of their special solution structure, xanthans – polysaccharides produced by fermentation – are favourably suited for use in the further exploitation of petroleum reservoirs (polymer flooding). Field trials have already shown good results [23, 44]. The flooding with pure water ceases to be economically efficient once the oil content of the water-oil mixture has dropped to 2%. In polymer flooding a quantity of polymer solution equal to about half the pore volume of the reservoir is injected which is then followed by twice this quantity of water. The benefits of EOR are heaped 1 to 2 years after the polymer programme has been commenced. So far only polyacrylamide-co-acrylates have been used [27], which, however, necessitate special requirements being made of the petroleum reservoirs. At high salt concentrations, of bivalent salts especially, polyacrylamide-co-acrylates are precipitated, so that the reservoir has to be preconditioned with fresh water. Non-ionic polyacrylamides are unable to fulfil the minimum viscosity requirement ($\eta_0 = 10 \text{ mPa} \cdot \text{s}$ at $c_p = 0.1\%$), even if extremely high molecular weights are employed [17]. In contrast to this, the exopolysaccharide xanthan, produced by the bacterium *Xanthomonas campestris* and first isolated and characterized by JEANES 1961, exhibits the following advantages [21, 39, 18, 31, 33].

- high stability in the presence of monovalent and bivalent ions
- high temperature resistance
- high shear stability in porous media
- high viscosity level at low polymer concentrations

These are the principal arguments which are repeatedly quoted for the application of xanthan in enhanced oil recovery, and which should enable a favourable mobility ratio to be achieved.

Laboratory experiments have recently been carried out for a field trial at a reservoir in North Germany with a high salt content (220 g/l TDS) and a temperature of 56°C, where it was found that xanthans from various producers differ markedly from each other with respect to their suitability for enhanced oil recovery [14]. For this field trial, fermentation broths were employed in concentrations of 2 to 3%. The solutions were then diluted and injected into the reservoir in quantities of approximately 100 m³/d with a xanthan content of 500 ppm. The results obtained for viscosity level and injectability from the investigations exhibited distinct differ-

ences not only between samples from different producers, but also between different batches from the same producers. It is therefore the aim of this work to characterize xanthans, particularly at low concentrations, and to work out an explanation for the differing macroscopic properties.

2. Experimental

The investigations included both commercially available xanthans as well as those synthesized in the laboratory. The commercial xanthans were kindly placed at our disposal by the manufacturers, and the laboratory xanthans by the Gesellschaft für Biotechnologische Forschung GmbH, GBF, in Braunschweig.

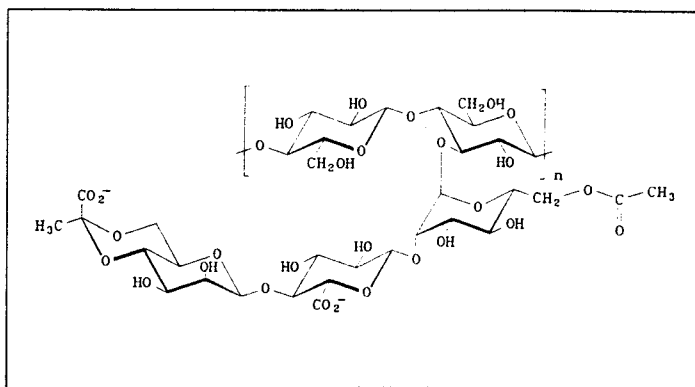


Fig. 1: Structural formula of the biopolymer xanthan according to Jansson

The acetate and pyruvate contents of the xanthans were measured according to an enzymatic standard test from the Boehringer company in Mannheim. The NMR spectroscopic determination of the acetate and pyruvate contents was carried out at 90°C in D₂O on a Bruker MSL 300 spectrometer. The spectra were recorded at a transmission frequency of 300.13 MHz with 256 scans in each case, with a relaxation delay of 10 s and 16 K data points. The molecular masses were determined by SEC [14]. The viscometric measurements for determining the intrinsic viscosity

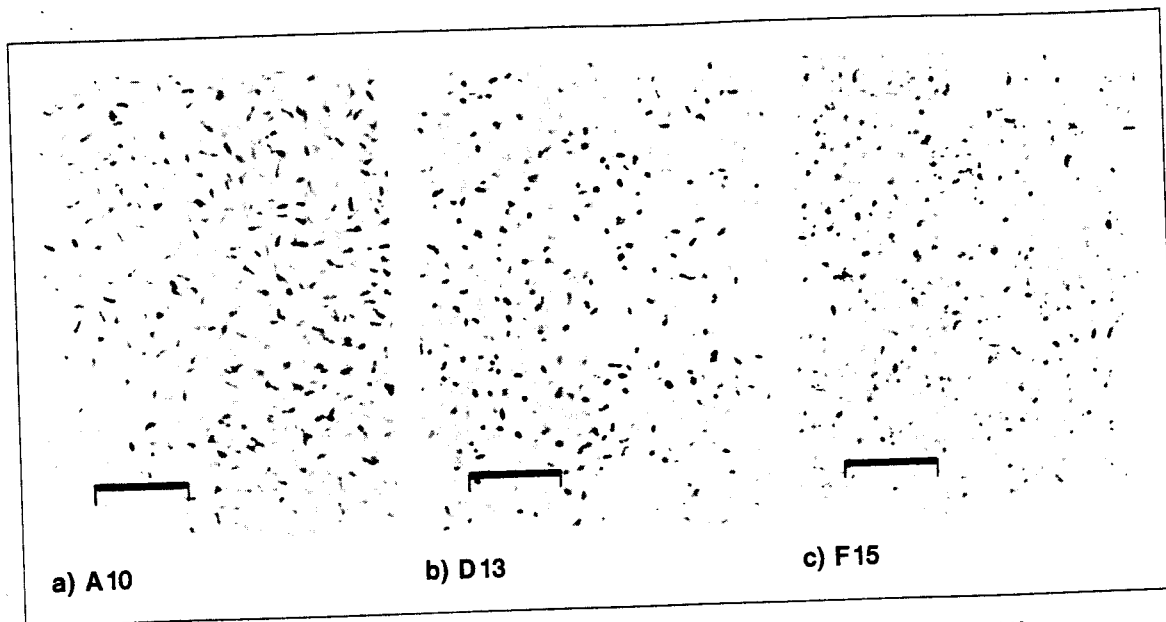


Fig. 2: Photomicrographs of xanthan A 10 (a), D 13 (b), F 15 (c) with the dead bacteria. The bars indicates a length of 10 μ

were performed using Ubbelohde viscometers and a Zimm-Crothers viscometer, thermostatically regulated at 25°C. Flow curves were carried out on rotary viscometers. The xanthan fermentation broths were obtained in various concentrations. The solutions for the injection tests were first diluted to approx. 5000 ppm, then subjected to shear, added to the reservoir water (220 g/l TDS), and then subjected to shear once more. The injection tests were carried out on a sandpack of the following specifications:

sand:	quartz sand	diameter:	1,9 cm
grain size:	63–90 μ m	porosity:	50–55 %
length:	4 cm	permeability:	2–3 μ m ²

After the injection test the R_{rf} value (residual resistance factor) was recorded by flooding with water. The R_{rf} value should lie between 1 and 3 for a good polymer [22]. Xanthan solutions both with and without bacteria were used for carrying out the injection measurements. In fig. 2 photomicrographs of three different xanthan samples are shown. The photomicrographs of a xanthan fermentation broth show that the bacteria can constitute a large proportion of the broth. Furthermore, the shape of the dead bacteria can vary significantly.

3. Results and discussion

In preliminary trials, conducted on a laboratory scale, the viscosity level, which is a decisive factor in the mobility behaviour within the reservoir, was examined for the various xanthan samples from different manufacturers. The viscous properties were investigated while paying particular attention to M_w or P_w , and it was found that a significant factor is whether the measurements have been carried out in the Newtonian or non-Newtonian region. Apart from the viscosity level, a very important role is also played by the injectability of the xanthan solutions during polymer flooding. As already mentioned by Lund [26] among others, poor injectability is brought about by a high aggregate content of the solution, which is reflected in high Huggins constants. A high aggregate content is not desirable as, apart from blockage of the reservoir, loss of polymer also occurs. Loss of polymer results in a deterioration of the mobility ratio and, therefore, a lower degree of oil extraction. In the light of these differing properties of xanthan it was deemed necessary to conduct a detailed comparative investigation into the flow behaviour, with particular emphasis on the structural parameters.

3.1. Viscosity yield

When an oil reservoir is flooded, it is generally assumed that the flow rates are equivalent to shear rates of approximately 1–10 s⁻¹, depending on the porosity and permeability [22]. For this reason, the viscosity level in Fig. 3 a is indicated by the xanthan concentration which is necessary to generate a viscosity of 16 mPa*s at a shear rate of 7.3 s⁻¹. As well as distilled water, a reservoir brine and a 210 g/l solution of NaCl were used as solvents. SANDFORD [33] found that xanthans with a high pyruvate content have higher viscosities. This can obviously be explained by the fact that the ultra-high molecular weight commercially-available xanthans often have higher pyruvate contents (Fig. 3b). The same

relationships result when the degree of polymerization is plotted as a function of the pyruvate content.

To ensure the comparability of the results in Fig. 3, the measurements at a shear rate of 7.3 s⁻¹ should be examined to examine whether they were all taken in the Newtonian range. Sample S1, with the highest intrinsic viscosity was therefore chosen for this examination (Table I). As can be seen from Fig. 4, the determination of the zero-shear-viscosity in the concentration range chosen was only possible at 68 ppm. Here, the Newtonian flow range is to be found at a shear rate of $\dot{\gamma} < 50$ s⁻¹. However, it can be clearly observed that xanthan readily fulfils the requirement for a shear rate of 10 s⁻¹ at 1000 ppm. The η_0 values can be calculated [3, 16], provided only that the $[\eta]$ -M relationship is known and that at least one measurement is taken in the Newtonian region. One result of this molecular model, among others, is that a structure-property relationship can be firmly established between the zero-shear-viscosity, the molecular weight and the concentration (η_0 - M_w -c relationship). In 1985, on the basis of this molecular model, Milas *et al.* [28] propounded this relationship. Using Milas' data, the resultant zero-shear-viscosity for xanthan S1 can be calculated. Unfortunately, as one can see, there is no agreement between the theoretical and measured values. On the contrary, it would seem to indicate that the xanthan sample S1 exhibits substantially higher η_0 values with respect to the concentration. Reasons which may be put forward for these differences are a variation in the molecular weight distribution and in the structure of the xanthan. These deviations illustrate that the solution properties of one xanthan cannot be applied to another xanthan.

3.2. Injectability

The polymers used in enhanced oil recovery must be resistant to the salt contained in the reservoir. Precipitation of the polymer due to the salt content must be avoided at all costs as this would lead to blockage of the rock pores. Another extremely important factor in this context is the proportion of aggregates in the xanthan solution, as these can also cause blockage of the rock pores. The occurrence of aggregates in native xanthan results in unusually high molecular weights in light scattering determinations. Holzwarth [12] thus states that the aggregates consist of up to 40 sub-units. The Huggins constants, obtained while determining the intrinsic viscosity (see Equation in Section 3.3), are a measure of the intermolecular interactions and thus of the proportion of aggregates in the solution. For non-aggregative, rod-like molecules the theoretical value of k_H is 0.4. Huggins constants above 0.4 indicate a higher level of intermolecular interactions, which are believed to result in aggregate formation. The extent to which aggregates are present in xanthan solutions can be determined by the pressure drop in filtration tests [26]. Alternatively, however, the Huggins constants of filtered and unfiltered solutions may also be determined.

Figure 5 clearly shows that the determination of the Staudinger index is barely dependent upon the aggregate content. Native xanthan molecules, which occur as double helices, have a length of approx. 2 μ m, whereas aggregates may be as long as 10 μ m [12]. These dimensions tally with the result. An 8 μ m filter thus causes a change in the k_H value from 3.34 (unfiltered) to 1.8, which may

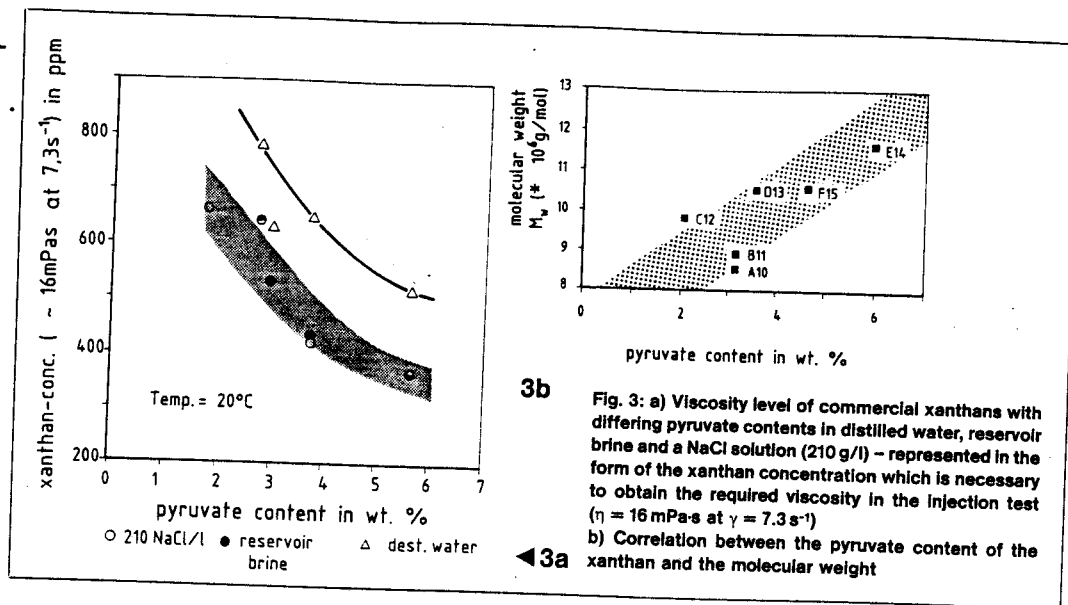


Fig. 3: a) Viscosity level of commercial xanthans with differing pyruvate contents in distilled water, reservoir brine and a NaCl solution (210 g/l) - represented in the form of the xanthan concentration which is necessary to obtain the required viscosity in the injection test ($\eta = 16 \text{ mPa}\cdot\text{s}$ at $\gamma = 7.3 \text{ s}^{-1}$) b) Correlation between the pyruvate content of the xanthan and the molecular weight

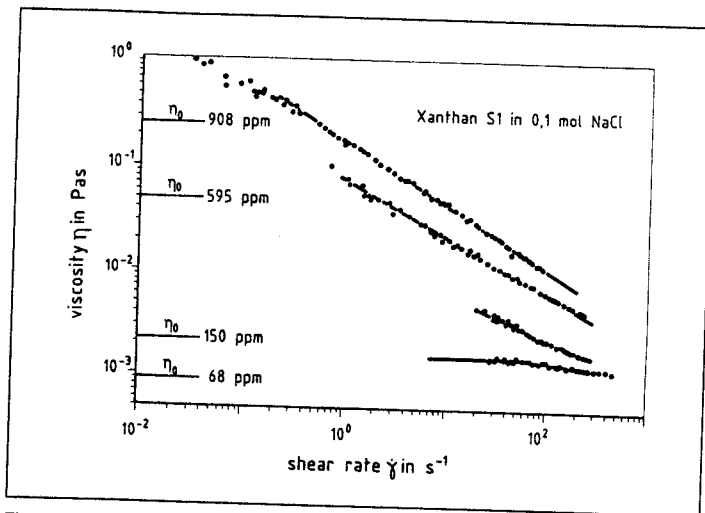


Fig. 4: Shear rate dependence of the viscosity of dilute xanthan solutions at 25 °C in comparison to the calculated zero-shear-viscosities of MILAS

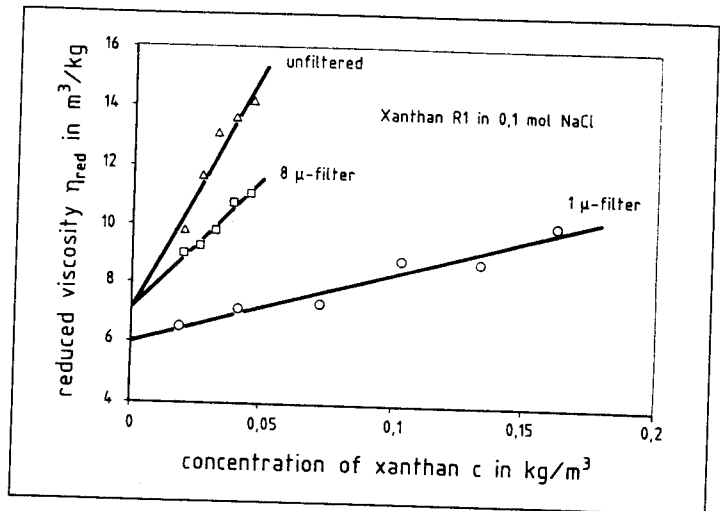


Fig. 5: Estimation of the aggregate content and thus the ease of filtration of a xanthan solution R1, by using different pore sizes in the determination of the Staudinger index ($T = 25 \text{ }^\circ\text{C}$; 8 μ cellulose nitrate filter from Sartorius and 1 μ regenerated cellulose filter from Schleicher & Schuell)

possibly be attributable to partial separation of very large aggregates, or to aggregates shattering. When a 1 μm filter is used k_H falls to 0.67 and the intrinsic viscosity simultaneously decreases by approx. 15%. This can be explained, in agreement with the results of Lund [25], by a significant loss of polymer during filtration. The loss of polymer became noticeable because of resistance during filtration and a residue on the filter. The injection measurements showed that the content of bacterial residues has no influence on the injectability of the polymer solutions. The

same was found for the influence of molecular weight [14]. These results infer that the reason for poor or good injectability of polymer solutions, and therefore their suitability for enhanced oil recovery, should be sought in the different structural properties of the xanthan molecule. Essential factors for the injectability seem to be the configuration of the molecule, the proportion of anionic groups and their location within the molecule, as this has an effect on aggregate formation, as already seen in Section 3.1.

Table I: Compilation of xanthans with differing microstructures

sample	C_{py} % w/w	C_{ac} % w/w	solvent	T °C	$[\eta]$ cm ³ /g	k_H	$k_H[\eta]^2$ (cm ³ /g)/10 ⁶	M_w^{**} 10 ⁶ g/mol
A 10	3.13	5.34	salt water*	25	4034	0.95	15.37	8.5
B 11	3.13	5.34	salt water*	25	5661	0.32	10.37	8.9
C 12	2.07	0.90	salt water*	25	3653	0.45	6.03	9.8
D 13	3.53	4.88	salt water*	25	7375	0.44	24.16	10.5
E 14	6.00	2.08	salt water*	25	8157	0.35	23.21	11.6
F 15	4.65	3.66	salt water*	25	9824	0.19	18.15	10.6
G 16			salt water*	25	5252	0.28	7.28	10.0
H 17			salt water*	25	3318	0.66	7.23	8.5
I 18			salt water*	25	1967	3.23	12.50	7.0
P 1	6.12	4.54						
S 1	4.42	3.90	0,1 M NaCl	25	10750	0.72	83.21	-
R 1	3.18	4.18	0,1 M NaCl	25	7075	3.34	167.2	-
K 1	3.30	4.33	0,1 M NaCl	25	5930	0.34	11.96	-
G 1	3.69	3.28	0,1 M NaCl	25	4951	0.65	15.93	-

*) reservoir water 220 g/l TDS

**) measurements from KLEINITZ et. al. 1989

3.3. Determination of the intrinsic viscosity

In determining the intrinsic viscosity, the reduced viscosity is normally plotted against the polymer concentration. The intercept of the ordinates then gives the Staudinger index.

$$\eta_{red} = [\eta] + k_H \cdot [\eta]^2 \cdot c$$

The above equation is an exponential series which has been truncated after the second term. The intercept of the ordinates for infinitely small concentrations then presents an indirect measure of the molecular weight, whereas the slope of the reduced viscosity as a function of the concentration is a direct measure of the thermodynamic quality of the solvent. Capillary viscometers are often used to determine these two values as they permit the viscosity to be measured with a very high degree of accuracy. It can be seen, however, that the Staudinger index of xanthan

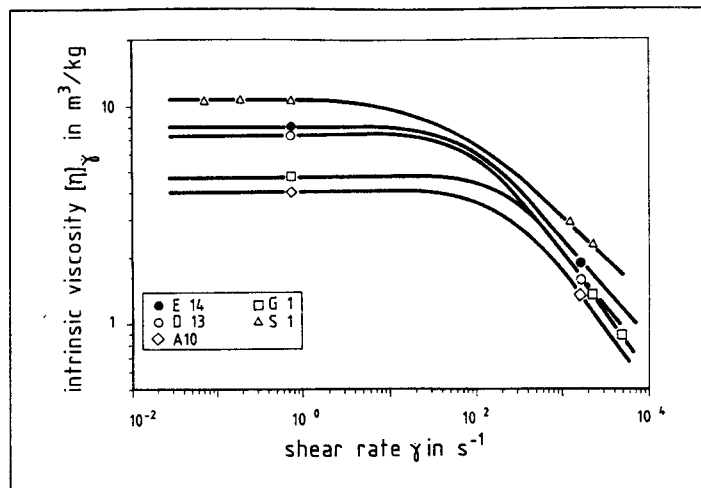


Fig. 7: Influence of the shear viscosity on the determination of the Staudinger Index for xanthans of different microstructures at 25°C

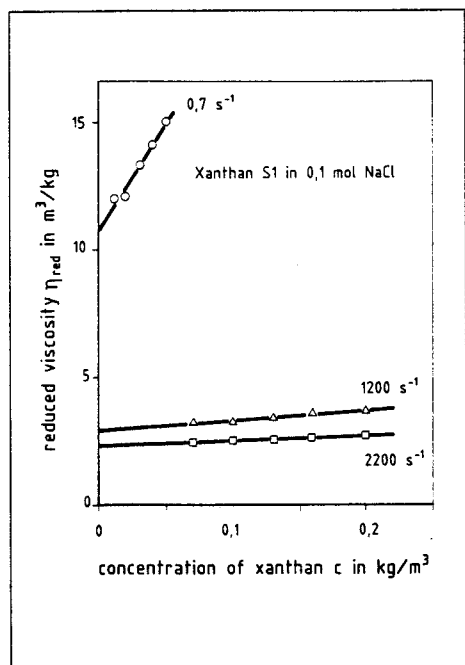
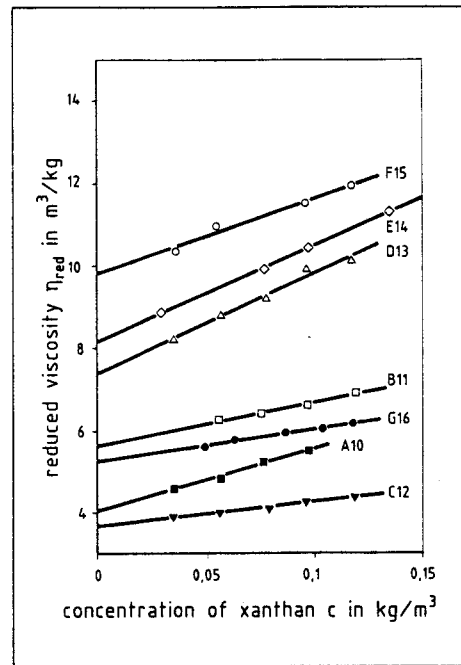


Fig. 6: Dependence of the shear viscosity on the measuring apparatus for dilute solutions of an ultra-high molecular weight xanthan S1 at 25°C (Zimm-Crothers viscometer $\dot{\gamma} = 0.7 \text{ s}^{-1}$, capillary viscometer $\dot{\gamma} = 1200$ and 2200 s^{-1}). ▶

Fig. 8: Influence of concentration on the zero-shear-viscosity of xanthan solutions in reservoir water at 25°C (according to Huggins equation) ▶▶



cannot be determined in a capillary viscometer as the shear rates occurring are too high. There is a discrepancy factor of 4 or 5 between intrinsic viscosities measured with a capillary viscometer and those measured with a Zimm-Crothers viscometer (see Fig. 6). The gradient of the straight lines $k_H[\eta]^2$ increases sharply with decreasing shear rate.

In addition, the reduced viscosity η_{red} also has to be extrapolated to $\dot{\gamma}$ against 0. To determine the intrinsic viscosity of the xanthan S1 in the capillary viscometer, concentrations of 50 to 200 ppm were necessary. Fig. 4, however, shows that the shear rates occurring in the capillary viscometer are located in the non-Newtonian region. If the recorded values of the intrinsic viscosities are plotted against the shear rate in the measuring head with a logarithmic scale on both axes, then a curve is obtained with the same shape as the flow curve.

The xanthan (S1) with the highest intrinsic viscosity exhibits a region independent of shear rate up to approx. 5 s^{-1} . If higher shear rates are used in determining the Staudinger index, an erroneous result is to be expected. If an $[\eta]$ -M relationship were then employed, too low a molecular weight would then result from the calculation. It would therefore seem necessary to conduct viscosity measurements on dilute xanthans in the region of the zero-shear-viscosity in measuring apparatus which only use very small shear rates.

The intrinsic viscosities of commercially-available xanthans for use in petroleum reservoirs were determined with a Zimm-Crothers viscometer.

Figure 8 shows that the Staudinger index, and with it the viscosity level too, of different xanthans can vary by a factor of 3. The different injectability is also reflected in the differing slopes $k_H[\eta]^2$,

and thus in the k_H value (Section 3.2.). k_H can assume unusually high values. *Launay* [19] reported a k_H value of 6.0 for a commercially-available xanthan in a 2% NaCl solution. Such great differences make it difficult to choose a xanthan for a particular field of application. These results are summarized in Table I, from which it can be clearly seen how greatly the xanthans deviate from one another in their properties.

One of the most important methods of characterization is the determination of the intrinsic viscosity, which allows a mean value of the molecular weight of the polymer to be obtained from viscometric measurements which are relatively easy to carry out via a calibration relationship from *Mark-Houwink-Sakurada*.

$$[\eta] = K_\eta \cdot M^a$$

$$c \rightarrow 0 \text{ and } \dot{\gamma} \rightarrow 0$$

If the Staudinger index $[\eta]$ of the polymer sample is plotted against the molecular weight with a logarithmic scale on both axes, the intercept of the ordinates gives K_η and the gradient the exponent a . These calibration relationships are, in each case, only valid for any one solvent at a given temperature for samples with equal molecular weight distribution. In the case of xanthan, a study has been made of the published material relating to this calibration relationship, the results of which are presented in Table II.

The list of published Mark-Houwink relationships from 1978 to the present shows how great an interest there is in xanthan. From Table 2 it can be clearly seen how sharply the K_η values and the exponents a both fluctuate. Values of 0.9 to 1.4 are found for the exponent a , which can be regarded as a measure of the thermodynamic quality of the solvent and thus provides a description of the solution configuration. Exponent a can assume values between 0 and 2. A value of 0.5 describes a pseudo-ideal state, in

Table II: Published $[\eta]$ -M relationships for xanthans as a function of the degree of substitution of acetate and pyruvate, salt content of the solution and temperature covering the period of time 1978-1990

K_η	a	M_w	Ac	Py	T °C	solvent NaCl	
$3,21 \cdot 10^{-5}$	1,25	$2 \cdot 10^5 - 4 \cdot 10^6$		0,4	25	0,1 M	Sho 1986
$4,64 \cdot 10^{-6}$	1,41	$\leq 2,5 \cdot 10^5$			25	0,1 M	Sato 1984
$4,41 \cdot 10^{-4}$	1,07	$\geq 1 \cdot 10^6 - 7,5 \cdot 10^6$			25	0,1 M	Sato 1984
$2,1 \cdot 10^{-3}$	0,90	$1,5 \cdot 10^6 - 10^7$				0,05 M Na_2SO_4	Müller 1988
$6,3 \cdot 10^{-3}$	0,93	$10^6 - 5 \cdot 10^6$		1	30	5 g/l	Muller 1984
$3,5 \cdot 10^{-5}$	1,244	$4,2 \cdot 10^4 - 3,3 \cdot 10^6$	1	0,6-1	25	0,1 M	Milas 1986
$1,52 \cdot 10^{-5}$	1,32	$3,3 \cdot 10^5 - 3,3 \cdot 10^6$	1	1	25	0,1 M	Milas 1986
$9,3 \cdot 10^{-5}$	1,20	$6,5 \cdot 10^5 - 7 \cdot 10^6$	0,48	0,36	25	0,1 M	Callet 1987
$1,72 \cdot 10^{-4}$	1,14	$3 \cdot 10^5 - 10^7$			25	0,1 M	Tinland 1989
$1,7 \cdot 10^{-4}$	1,14	$3 \cdot 10^5 - 7 \cdot 10^6$	0,75	0,4	25	0,1 M	Milas 1985
$2,4 \cdot 10^{-4}$	1,10	$3 \cdot 10^5 - 1 \cdot 10^6$			25	0,1 M NaNO_3	Tinland 1988
$9,41 \cdot 10^{-4}$	0,956	$1,5 \cdot 10^6 - 10^7$	0,62	0,48	25	0,1 M NaCl	Ach 1987
$5,66 \cdot 10^{-4}$	1,0	$3 \cdot 10^5 - 10^7$			25	0,3 M	Tinland 1989
$1,72 \cdot 10^{-4}$	1,14	$3 \cdot 10^5 - 10^7$			25	0,1 M	Tinland 1989
$4 \cdot 10^{-5}$	1,23	$3 \cdot 10^5 - 10^7$			25	0,03 M	Tinland 1989
$3,14 \cdot 10^{-5}$	1,26	$3 \cdot 10^5 - 10^7$			25	0,01 M	Tinland 1989
$2,83 \cdot 10^{-5}$	1,27	$\leq 2 \cdot 10^5$			25	0,01 M	Liu 1987
$5,71 \cdot 10^{-5}$	1,21	$2 \cdot 10^5 - 10^6$			25	0,01 M	Liu 1987
$2,57 \cdot 10^{-4}$	1,09	$\leq 2 \cdot 10^5$			80	0,01 M	Liu 1987
$1,82 \cdot 10^{-3}$	0,93	$2 \cdot 10^5 - 10^6$			80	0,01 M	Liu 1987
$1,64 \cdot 10^{-5}$	1,29	$1 \cdot 10^5 - 1 \cdot 10^6$		0,34	25	0,01 M	Zhang 1987
	1,35	$\leq 1 \cdot 10^6$			20	0,75 M	Holzwarth 1978
	0,96	$\geq 1 \cdot 10^6$			20	0,75 M	Holzwarth 1978

which the polymer is present as a statistical coil in the solution. The greater the exponent is, the more stiffly the polymer behaves in the solution. If a is 2, an ideal rod exists [18]. The different samples for preparing a $[\eta]$ -M relationship should represent an homologous series with respect to their molecular weight distribution and type and frequency of branching. The published list of relationships is based on samples obtained by the enzymatic or mechanical degradation of native xanthan samples. Mechanical degradation is often brought about by ultrasound, which inevitably results in samples of differing distribution widths. Enzymatic degradation is associated with a change in the substitution degree of acetate and pyruvate [28]. In plots with a logarithmic scale on both axes, curves are often obtained, so that the $[\eta]$ -M relationships are only valid for a limited range of molecular weights. The gradient is significantly steeper for small molecular weights than for very high ones. In principle, there are 3 causes for the curved graph. Changes in the type and frequency of branching, which cannot in principle be excluded, lower the hydrodynamic volume and consequently the Staudinger index of the sample, although the molecular weight remains the same [15]. A curve can also be caused by differing molecular weight distributions in the samples. The semi-flexible nature of the xanthan molecule [45] may possibly be put forward as the third explanation for the varying gradient in the plot of the Staudinger index as a function of the molecular weight. Small molecular weights exhibit high exponents, up to 1.41, due to their high stiffness, whereas the xanthan becomes more flexible with increasing chain length, which is shown in a lowering of the a value. At very high molecular weights exponent a decreases to 0.9. The comparability of the $[\eta]$ -M relationships is also made difficult by the frequent absence of data for the degree of acetate and pyruvate substitution. Table I gives the results for the enzymatic determination of the acetate and pyruvate contents of some xanthan samples. For some samples this determination was not only carried out enzymatically, but also by means of NMR spectroscopy. In order to obtain good ^1H -NMR spectra from xanthan, the samples must be purified and the remaining water substituted for deuterium oxide. First investigations lead to the conclusion that ultrasonic degradation of the xanthan samples makes the determination of the degree of substitution more precise due to better resolution. In addition, the spectra must be recorded at 90°C, because at this temperature the xanthan which

is present in the denatured form has a significantly greater signal intensity than either the native or renatured form. If attention is paid to the appropriate measuring conditions, the signals in the spectrum can be assigned to the acetate and pyruvate groups (fig. 9). The quantitative evaluation makes use of the only α -anomeric proton in the xanthan molecule, which occurs in the side chain [32]. Taking the ratio of the areas of these signals then gives the acetate and pyruvate content of the xanthans. The results recorded by this method show good agreement with those from the enzymatic determination. The results stated go to show that the contents of individual xanthans differ, and that not all of the side chains in a xanthan molecule contain acetate and pyruvate groups.

Sandford [33] observed in 1978 that the fractional precipitation of xanthan with ethanol results in fractions with differing pyruvate contents. This is contrary to the findings of a recent BMFT research project which took place at Henkel, and which established that although a low-molecular weight xanthan is initially formed in the fermentation, the acetate and pyruvate content remain constant throughout the entire reaction period. Removal of samples of the xanthan fermentation broth at different intervals during the reaction represents in principle another method of obtaining a homologous series. Different fermentation conditions and processing techniques will of course occur amongst the selection of xanthans from various companies. For instance, the choice of nitrogen source as the nutrient for the bacterium has a decisive influence on the solution properties of the xanthan [25]. The presence of the L-amino acid methionine during the fermentation impedes the production of xanthan from the bacterium, whereas other amino acids result in increased production [8]. If the flow curves of different xanthans are recorded, overlapping of the material functions is observed, which can only be explained by different solution structures. Furthermore, the Mark-Houwink exponent of the xanthan is also influenced by changes in salt concentration and temperature. Comparability of the calibration relationship is therefore made difficult.

Conclusions

It is not unusual for polysaccharides to form helical structures. Thus xanthan forms a double helix whereas other polysac-

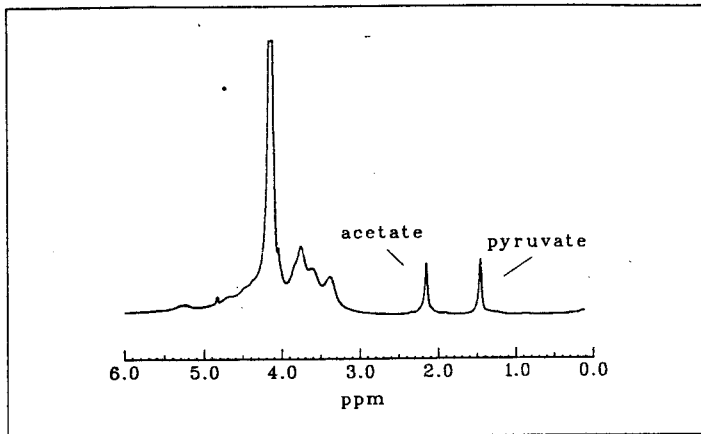


Fig. 9: $^1\text{H-NMR}$ -spectra of xanthan S1 in D_2O at 90°C

charides, such as scleroglucan are capable of forming triple helices [46]. The xanthan helix is a semiflexible and not a completely rigid polymer as can be shown by electron microscopy [40]. Native xanthan, which has molecular weights significantly in excess of 10^6g/mol , is produced by the classic method, in a fermenter. The high viscosities which arise from this method cause a restriction of the oxygen supply, which can be strongly influenced by the mixing technique. This oxygen restriction not only reduces the productivity of the bacterium, but also causes a drop in the molecular weight of the xanthan formed. Poor mixing with local differences in the oxygen distribution may have such an influence on the polydispersity [41]. To avoid these problems at high viscosities, emulsion polymerizations have recently become the subject of investigations concerning the manufacture of xanthans. Though, even here the choice of the agitation system plays an important role [7]. The differences in the macroscopic behaviour of xanthans, which occur both between samples and between manufacturers, cannot be caused by the diversities in manufacturing and processing techniques alone, but also directly by the composition of the copolymers, with respect to their frequency and distribution along the chain. Published material concerning the influence of the acetate and pyruvate groups on the material properties is subject to some controversy. Studies conducted by Callet [4] and Bradshaw [2] have shown that the degree of substitution has no influence on the viscosity. In contrast to this, however, Sloneker [37] has reported that removal of the acetate groups causes an improvement in the physical properties, such as higher viscosities in the presence of salts, and in the manufacture of more flexible films. Cheetham [5], Smith [38] and also Lecourtier [21] claim that association with salts takes place, particularly for xanthans with a high pyruvate content, which result in a sharp increase in viscosity, or even precipitation of the xanthan. However, it is certain that the pyruvate groups destabilize the helix due to electrostatic repulsion, whereas the acetate groups stabilize the helix by intramolecular hydrogen bonds [6, 10]. The degree of acetate and pyruvate substitution is therefore able to influence the solution structure. The temperature of the transition from the ordered to the disordered state is not only determined by the salt content and nature of the cations [9] in the solution, but also by the degree of substitution. The irreversible splitting of the double helix into a single helix in distilled water has thus so far only been observed for a xanthan with a pyruvate content of 100% (with respect to the side chain) [20]. If one solution structure is transformed into another, the solution properties also change. The wide-ranging investigations carried out on xanthan to date infer that it is a copolymer consisting of 4 monomeric units which occur in the molecule in varying proportions. A structural formula such as that shown in fig. 1 therefore represents a crude simplification. The structural configuration of xanthan is considerably better represented by Fig. 10 although this formula is also unable to specify the sequence of the side chains. In addition, there is still no proof that the side groups are regularly bonded to every second glucose unit of the main chain.

This work was kindly supported by the European Community (EC) and by the Bundesministerium für Forschung und Technologie (BMFT).

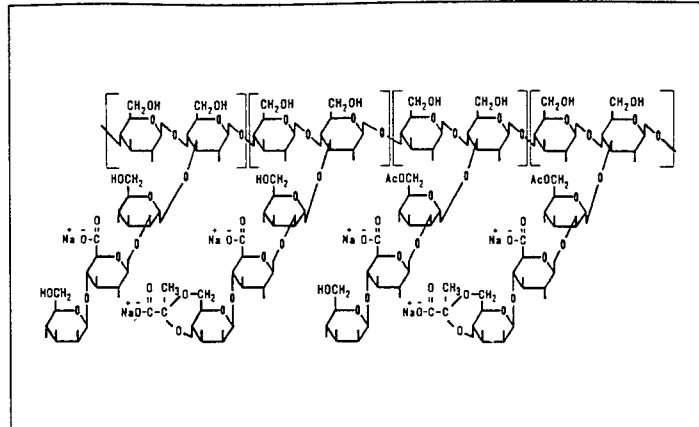


Fig. 10: Structural formula of the xanthan copolymer

References

- [1] A. Ach: Dissertation, Braunschweig 1987
- [2] I. J. Bradshaw, B. A. Nisbet, M. H. Kerr, I. W. Sutherland: *Carb. Polym.* **3**, 23 [1983]
- [3] M. Bouldin, W.-M. Kulicke, H. Kehler: *Coll. & Polym. Sci.* **299**, 793 [1988]
- [4] F. Callet, M. Milas, M. Rinaudo: *Int. J. Biol. Macromol.* **9**, 291 [1987]
- [5] N. W. H. Cheetham, N. M. N. Norma: *Carb. Polym.* **10**, 55 [1989]
- [6] M. Dentini, V. Crescenzi, D. Blas: *Int. J. Biol. Macromol.* **6**, 951 [1984]
- [7] K. Franz: BMFT-Bericht 1987 Nr. PBE 03 8660
- [8] HENKEL KGaA: BMFT-Bericht 1987 Nr. 0386595
- [9] G. Holzwarth: *Biochemistry* **15**, 433 [1976]
- [10] G. Holzwarth: *Carb. Res.* **66**, 173 [1978]
- [11] G. Holzwarth, J. Ogletree: *Carb. Res.* **76**, 277 [1979]
- [12] G. Holzwarth, E. B. Prestridge: *Science* **197**, 757 [1977]
- [13] P. E. Jansson, L. Kenne, B. Lindberg: *Carb. Res.* **45**, 275 [1975]
- [14] W. Kleinitz, W. Littmann, H. Herbst: 5th European Symp. EOR, Budapest [1989]
- [15] W.-M. Kulicke, H.-H. Hörl: *Coll. & Polym. Sci.* **258**, 817 [1980]
- [16] W.-M. Kulicke, J. Klare: *Angew. Makromol. Chemie* **84**, 67 [1980]
- [17] W.-M. Kulicke, J. Klein: *Erdöl & Kohle, Erdgas-Petrochemie* **8**, 373 [1978]
- [18] W.-M. Kulicke, J. Lehmann: *Chem. Ing. Tech.* **12**, 967 [1986]
- [19] B. Launay, G. Cuvelier, S. Martinez-Reyes: in "Gums and stabilisers for the food industry" ed. G. O. Phillips, D. J. Weedlock, P. A. Williams; Oxford Pergamon Press p. 79 [1984]
- [20] J. Lecourtier, G. Chauveteau, G. Muller: *Int. J. Biol. Macromol.* **8**, 306 [1986]
- [21] J. Lecourtier, C. Noik, P. Barbey, G. Chauveteau: 4th European Symp. EOR, Hamburg [1987]
- [22] W. Littmann: *Polymer Flooding*, Elsevier, Amsterdam [1988]
- [23] W. Littmann, W. Kleinitz: BMFT-Statusreport 1988 Nr. 03 E-6022-A
- [24] W. Lui, T. Sato, T. Norisuje, H. Fujita: *Carb. Res.* **160**, 267 [1987]
- [25] T. Lund, R. Boreng: 14th Int. Carbohydr. Symp., Stockholm [1988]
- [26] T. Lund, R. Boreng, E. O. Bjornestad, P. Foss: 5th European Symp. EOR, Budapest [1989]
- [27] B. Maitin: 3rd European Symp. EOR, Rom [1985]
- [28] M. Milas, M. Rinaudo, B. Tinland: *Polym. Bull.* **14**, 157 [1985]
- [29] R. J. Müller, A. Ach, P. Schwarzer, J. Klein: *Proc. Makromol. Symp. Freiburg* 1988
- [30] G. Muller, J. Lecourtier, G. Chauveteau, C. Allain: *Makromol. Chem., Rapid Commun.* **5**, 203 [1984]
- [31] M. Rinaudo, M. Milas, E. Moan: *Europ. Polym. J.* **15**, 903 [1979]
- [32] M. Rinaudo, M. Milas, F. Lambert, M. Vincendon: *Macromolecules* **16**, 816 [1983]
- [33] P. A. Sandford, J. E. Pittsley, C. A. Knutson, P. R. Watson, M. C. Cadmus, A. Jeanes: *Am. Chem. So. Symp. Ser.* **45**, 192 [1977]
- [34] P. A. Sandford, P. R. Watson, C. A. Knutson: *Carb. Res.* **63**, 253 [1978]
- [35] T. Sato, S. Kojima, T. Norisuje, H. Fujita: *Polym. J.* **16**, 423 [1984]
- [36] T. Sho, T. Sato, T. Norisuje: *Biophys. Chem.* **25**, 307 [1986]
- [37] J. H. Sloneker, A. Jeanes: *Can. J. Chem.* **40**, 2066 [1962]
- [38] I. H. Smith, K. C. Symes, C. J. Lawson, E. R. Morris: *Int. J. Biol. Macromol.* **3**, 129 [1989]
- [39] G. Southwick, J. M. Jamieson, J. Blackwell: *J. Appl. Polym. Sci.: Appl. Polym. Symp.* **37**, 385 [1983]
- [40] B. T. Stokke, O. Smidsrod, A. B. L. Marthinsen, A. Esigaeter: in "Water-Soluble Polymers for Petroleum Recovery," ed. G. A. Stahl, D. N. Schulz; Plenum Press, New York p. 243 [1988]
- [41] I.-S. Suh, H. Herbst, A. Schumpe, W.-D. Deckwer: *Biotechn. Lett.* **12**, 201 [1990]
- [42] B. Tinland, J. Mazet, M. Rinaudo: *Makromol. Chem., Rapid Commun.* **9**, 69 [1988]
- [43] B. Tinland, M. Rinaudo: *Macromolecules* **22**, 1863 [1989]
- [44] A. Westerkamp, W. Crüger, W. Littmann, D. Menz: BMFT-Statusreport 1985 Nr. 03 E-6022-A
- [45] H. Yamakawa, M. Fujii: *Macromolecules* **9**, 128 [1974]
- [46] T. Yanaki, T. Norisuje: *Polym. J.* **15**, 389 [1983]
- [47] L. Zhang, W. Liu, T. Norisuje, H. Fujita: *Biopolymers* **26**, 333 [1987]